Transgenic Res (2012) 21:439–447
DOI 10.1007/s11248-011-9539-1

TECHNICAL REPORT

Comprehensive application of an mtDsRed2-Tg mouse strain for mitochondrial imaging

Junya Yamaguchi · Satoshi Nishiyama · Midori Shimanuki · Tomio Ono · Akitsugu Sato · Kazuto Nakada · Jun-Ichi Hayashi · Hiromichi Yonekawa · Hiroshi Shitara

Received: 16 May 2011 / Accepted: 11 July 2011 / Published online: 27 July 2011

Abstract Mitochondria are essential for many cellular functions such as oxidative phosphorylation and calcium homeostasis; consequently, mitochondrial dysfunction could cause many diseases, including neurological disorders. Recently, mitochondrial dynamics, such as fusion, fission, and transportation, have been visualized in living cells by using time-lapse imaging systems. The changes in mitochondrial morphology could be an indicator for estimating the activity of mitochondrial biological function. Here, we report a transgenic mouse strain, mtDsRed2-Tg, which expresses a red fluorescent protein, DsRed2, exclusively in mitochondria. Mitochondrial morphology could be clearly observed in various tissues of this strain under confocal microscope. Recently, many transgenic mouse strains in which enhanced green fluorescent protein (EGFP)-tagged proteins of interest are expressed have been established for physiological analysis in vivo. After mating these strains with mtDsRed2-Tg mice, red-colored mitochondria and green-colored proteins were detected simultaneously using fluorescent imaging systems, and the interactions between mitochondria and those proteins could be morphologically analyzed in cells and tissues of the F_1 hybrids. Thus, mtDsRed2-Tg mice can be a powerful tool for bioimaging studies on mitochondrial functions.

Keywords Mitochondria · DsRed2 · EGFP · Transgenic mice · Imaging

Electronic supplementary material The online version of this article (doi:10.1007/s11248-011-9539-1) contains supplementary material, which is available to authorized users.

J. Yamaguchi · S. Nishiyama · M. Shimanuki · T. Ono · H. Yonekawa · H. Shitara (✉)
Laboratory for Transgenic Technology, Tokyo Metropolitan Institute of Medical Science, 1-6, Kamikitazawa 2-chome, Setagaya-ku, Tokyo 156-8506, Japan
e-mail: shitara-hr@igakuken.or.jp

J. Yamaguchi · S. Nishiyama · A. Sato · K. Nakada · J.-I. Hayashi · H. Yonekawa · H. Shitara
Graduate School of Life and Environmental Sciences, University of Tsukuba, Ibaraki 305-8572, Japan

Introduction

Mitochondria are major centers of both energy production and many biological functions such as apoptosis signaling and calcium storage (Kroemer and Reed 2000; Rizzuto et al. 2000). Therefore, mitochondrial dysfunction causes many diseases, particularly neurological disorders (Chen and Chan 2006; Matsuda et al. 2010). Electron microscopic observations have indicated that mitochondria typically possess an oval shape. However, recent improvements in bioimaging techniques have revealed that mitochondria travel to a great extent in the cytoplasm by changing their morphology and that their morphology is cell-type specific (e.g., round, tubule, and extended reticular network-like forms). These morphological changes are

closely controlled by mitochondrial fusion, fission, and transportation (Chan 2006; Hermann and Shaw 1998; Hirokawa 1998; Yaffe 1999). Mitochondrial fusion and fission in mammalian cells are regulated by several proteins, including optic atrophy type 1, mitofusins, and dynamin-related protein 1 (Chen et al. 2003; Griparic et al. 2004; Ishihara et al. 2009), which help to maintain mitochondrial function by exchanging mitochondrial components (Ono et al. 2001). Therefore, changes in mitochondrial morphology are thought to be linked to mitochondrial biological function.

Enhanced green fluorescent protein (EGFP) has been widely used for bioimaging in molecular and cellular biology (Shaner et al. 2005; Tsien 1998). We have previously generated transgenic (Tg) mice (mtGFP-Tg mice) in which EGFP is expressed exclusively in mitochondria (Shitara et al. 2001). mtGFP-Tg mice have facilitated observations of mitochondrial morphology in any tissue of interest without the use of complicated methods such as specific chemical staining for mitochondria (Shitara et al. 2010). Recently, many Tg mouse strains expressing an EGFP-labeled and/or EGFP-tagged protein have also been generated. For example, a Tg mouse strain, C57BL/6J-Tg (CAG-*Tfam*/EGFP) 38Rin (*Tfam*/EGFP-Tg mice), has been established to express the fusion gene of mitochondrial transcription factor A (*Tfam*) and EGFP (Nishiyama et al. 2010). TFAM is a known mitochondrial DNA (mtDNA)-binding protein (Chen and Butow 2005; Larsson et al. 1996) that packages mtDNAs into DNA–protein complexes called mitochondrial nucleoids (Alam et al. 2003; Chen and Butow 2005). Therefore, TFAM has been visualized and analyzed morphologically as mitochondrial nucleoids in cells of *Tfam*/EGFP-Tg mice. To simultaneously visualize mitochondria and mitochondrial nucleoids, we generated an alternative Tg mouse strain, C57BL/6J-Tg (CAG-Cox8/DsRed2)1Rin (mtDsRed2-Tg mice), expressing a mitochondrially targeted red fluorescent protein, DsRed2, under the control of the CAG enhancer/promoter (Niwa et al. 1991). Mitochondria could be visualized in all observed tissues of mtDsRed2-Tg mice, similar to those of mtGFP-Tg mice, under a confocal laser-scanning microscope. Then, we crossed mtDsRed2-Tg mice with *Tfam*/EGFP-Tg mice to simultaneously analyze the localization of mitochondria and mitochondrial nucleoids.

Here, we report the genetic characteristics of an mtDsRed2-Tg mouse strain and their application with a *Tfam*/EGFP-Tg mouse strain in tissue imaging. mtDsRed2-Tg mice enable simultaneous in vivo imaging of mitochondria and EGFP-tagged proteins to cross with Tg mouse strains expressing an EGFP-labeled and/or EGFP-tagged protein.

Materials and methods

Expression vector construction

The signal sequence of cytochrome *c* oxidase subunit VIII (*Cox8*) (GenBank U15541) was prepared from a previously constructed vector (Shitara et al. 2001). The coding region of DsRed2 was amplified by PCR with primers 5′-CAT GGA TCC ATG GCC TCC TCC GAG AAC G-3′ and 5′-TAC GAA TTC CTA CAG GAA CAG GTG GTG GCG-3′ using the recombinant plasmid pDsRed2-Mito (Clontech) as a template. *Eco*RI/*Bam*HI fragments of signal sequence and DsRed2 were ligated into pCAGGS expression vector digested with *Eco*RI.

Generation of Tg mice

All animal experiments were approved by the Institutional Animal Experiment Committee of Tokyo Metropolitan Institute of Medical Science. For mtDsRed2-Tg mice, DNA fragments for transgenesis were removed by double digestion with *Sal*I and *Bln*I, separated by agarose gel electrophoresis from the cloning vector, and then purified using a QIAquick Gel Extraction Kit (Qiagen). The purified DNA fragments were injected into the pronuclei of fertilized mouse (C57BL/6J, B6) oocytes according to the standard procedure. To identify Tg mice, genomic DNA was prepared from ear-punched pieces or tails, and a set of primer pairs, 5′-GAC CCA CAA GGC CCT GAA G-3′ and 5′-TGC TCC ACG ATG GTG TAG TCC-3′, was synthesized to amplify the PCR fragments (159 bp) specific for the Tg sequence. *Tfam*/EGFP-Tg mice were described previously (Nishiyama et al. 2010).

Sample preparation

Primary adherent cells from tail

mtDsRed2-Tg mouse tail samples were cut into approximately 1 mm in length and placed into a glass

base culture dish with DMEM (Sigma) containing 10% newborn calf serum. After culturing for 5 days, MitoTracker Green FM (Invitrogen) was added to this medium at a concentration of 500 nM. After incubation for 30 min at 37°C, primary adherent cells were washed twice and observed.

Frozen tissue sections

Adult male mice were anesthetized and perfused through the left chamber with 4% paraformaldehyde in PBS (PFA/PBS). Then, tissues were further fixed in 4% PFA/PBS overnight at 4°C. The fixed tissues were transferred to 15% sucrose in PBS for over 4 h and then to 30% sucrose in PBS for over 4 h at 4°C. The tissue samples were embedded in Tissue-Tek O.C.T. Compound (Sakura Finetek Japan) and subsequently frozen in liquid nitrogen. Frozen tissue sections were cut at a thickness of 8–10 μm with a cryostat (Leica) and collected on slide glasses. Frozen tissue sections were air-dried, washed with PBS, and mounted with Slow Fade Gold antifade reagent with 4′,6-diamidino-2-phenylindole (DAPI) (Invitrogen).

Fluorescence imaging

Fluorescence images were acquired with a confocal laser-scanning microscope (LSM510 META; Zeiss) equipped with a 100× (alpha Plan-Fluar) objective. DAPI signals were excited at 405 nm with a diode laser and obtained after passing through the 420–480 nm bandpass filter. MitoTracker Green FM signals were excited at 488 nm with an argon-ion laser and obtained after passing though the 505–530 nm bandpass filter. DsRed2 signals were excited at 543 nm with a HeNe laser and obtained after passing through the 560 nm longpass filter.

Histochemical analyses of cytochrome *c* oxidase (COX) and succinate dehydrogenase (SDH) activities

To examine mitochondrial respiration activity in tissues from Tg mice, COX (complex IV) and SDH (complex II) activities were examined by histochemical methods. The histochemical staining for COX activity was carried out as reported previously (Seligman et al. 1968). Briefly, air-dried cryosections (10 μm thick) were incubated in a reaction medium: diaminobenzidine tetrahydrochloride (DAB), 5 mg; sodium phosphate buffer (0.05 M, pH 7.4), 9 ml; catalase (20 μg/ml), 1 ml; cytochrome *c*, 10 mg; sucrose 750 mg. COX activity was visualized as a brown DAB reaction product. For histochemical staining to determine SDH activity, air-dried cryosections (10 μm thick) were incubated in a reaction medium: nitro blue tetrazolium (NBT), 30 mg; sodium succinate (0.2 M), 15 ml; phosphate buffer (0.2 M, pH 7.4), 15 ml. SDH activity was visualized as a blue NBT reaction product.

Results and discussion

DsRed2 and EGFP are easily distinguished by their distinct excitation and emission peaks (558 and 583 nm, respectively, for DsRed2 vs. 488 and 507 nm, respectively, for EGFP). Therefore, we selected DsRed2 as a fluorescent marker and constructed a DsRed2 expression vector to generate mtDsRed2-Tg mice.

Recent studies have presented mitochondrial imaging techniques using non-EGFP fluorescent proteins in specific cells in mice. For example, mitochondria can be observed with cyan fluorescent protein or yellow fluorescent protein in the axonal transport of neuronal cells (Misgeld et al. 2007) and with DsRed2 in the sperm cells (Hasuwa et al. 2010). To observe mitochondria in several tissues, DsRed2 cDNA expression was driven by the CAG enhancer/promoter (Niwa et al. 1991). The transgene contains the mitochondrial transit peptide of COX8; therefore, DsRed2 localized exclusively to the mitochondrial matrix (Rizzuto et al. 1995). Using these constructs, mtDsRed2-Tg mice were generated by pronuclear injection of the DNA construct in fertilized oocytes. The transgene was detected by PCR using specific primers for DsRed2, and we obtained 3 candidate founder mice transgenic for the mtDsRed2 gene. DsRed2 fluorescence was observed in founder #1, and large differences between individuals of offspring were not observed in the fluorescence intensity (Supplementary Fig. 1). We maintained the offspring of the founder #1 and used hemizygous mtDsRed2-Tg mice in the following analyses.

Then, we examined the localization pattern of DsRed2 in living cells to confirm whether fluorescence occurred exclusively in the mitochondria of mtDsRed2-Tg mice. In primary cultured adherent

cells derived from the tail of an mtDsRed2-Tg mouse strain, DsRed2 fluorescent signals were detected in the cytoplasm, and these signals exhibited mitochondria-typical morphology under confocal laser-scanning microscope. These cells were stained by MitoTracker Green FM and observed by confocal laser-scanning microscope; subsequently, these two images were merged, and the merged images demonstrated that DsRed2 was exclusively localized in the mitochondria (Fig. 1).

We next prepared frozen tissue sections to observe mitochondria labeled with DsRed2 in various tissues, including tissues from the heart, liver, stomach, cerebrum, cerebellum, ileum, colon, pancreas, and kidney of mtDsRed2-Tg mice by confocal laser-scanning microscope (Fig. 2). Mitochondria were easily observed in all examined tissues, but the expression level of DsRed2 differed among tissues. In cardiac muscle, mitochondria were visualized in a row in between myocardial fibers, and numerous mitochondria were located in these areas (Fig. 2a, b). No mitochondria were observed in non-Tg B6 mouse under the same imaging conditions as shown in Fig. 2b (Fig. 2c). In the liver, mitochondria were uniformly distributed in the cytoplasm of whole cells (Fig. 2d). In the gastric gland in the stomach, several different types of mitochondria could be observed in the cellular regions (Fig. 2e, f). Mitochondria in gastric parietal cells were shorter than those in basal cells of the gastric gland. High mitochondrial density was also observed in gastric parietal cells. This distribution is probably due to the high energy requirement for H^+/K^+-ATPase, which produces gastric acid (Sachs et al. 1976). In the hippocampus and cerebral cortex, numerous mitochondria were observed, and mitochondria in Purkinje cells of the cerebellum exhibited dense network-like forms (Fig. 2g, h, i and Supplementary Fig. 2). Recent studies have shown morphological abnormalities of mitochondria in neurodegenerative

Fig. 2 Confocal images of mitochondria in tissues from mtDsRed2-Tg mice. Mitochondria were visualized by DsRed2 (*red*) and counterstained for nuclei with DAPI (*blue*). **a** Longitudinal section of cardiac muscle fiber. **b** Transverse section of cardiac muscle fiber. **c** Transverse section of cardiac muscle fiber from a wild B6 mouse as a control for examining autofluorescence. **d** Liver. **e** The middle part of the gastric gland in the stomach. *Arrowheads* indicate parietal cells. **f** The base of the gastric gland in the stomach. **g** Hippocampus in the cerebrum. **h** Cerebral cortex in the cerebrum. **i** Molecular layer, Purkinje cell layer, and granule cell layer in the cerebellum. *Arrowheads* indicate Purkinje cells. **j** Intestinal villi of the ileum. **k** Mucosa of the colon. **l** Regions where DsRed2 signals were not uniform in intestinal villi of the ileum. **m** Acinar cell (*arrowhead*) and islet (*arrow*) in the pancreas. **n** Convoluted tubules (*arrowhead*) and glomerulus (*arrow*) in the kidney. *Scale bar* 10 μm

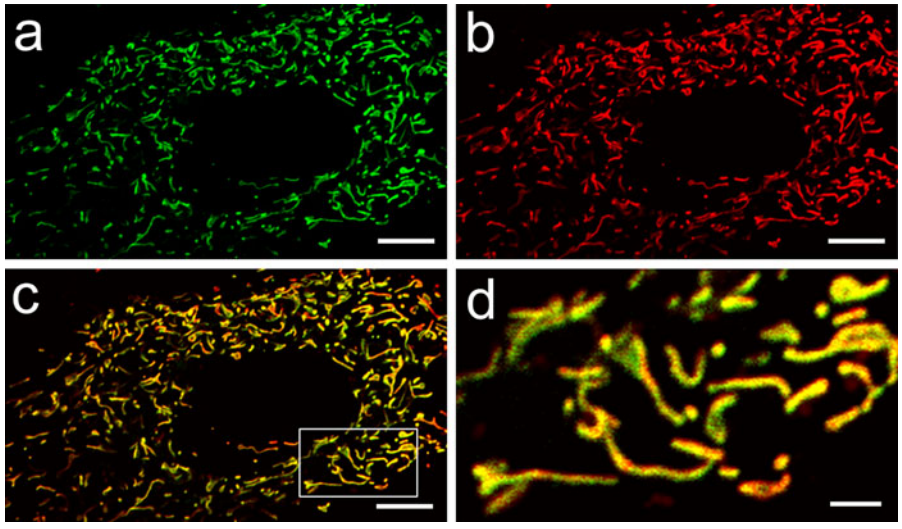

Fig. 1 Mitochondria were visualized by MitoTracker Green FM labeling and mtDsRed2 targeting. DsRed2 was specifically expressed in the mitochondria of primary adherent cells. **a** Fluorescence image of MitoTracker Green FM. **b** Fluorescence image of DsRed2. **c** Merged image of MitoTracker Green FM and DsRed2. The 2 signals overlapped. *Scale bar* 10 μm. **d** Magnified image from inset of (c). *Scale bar* 2 μm

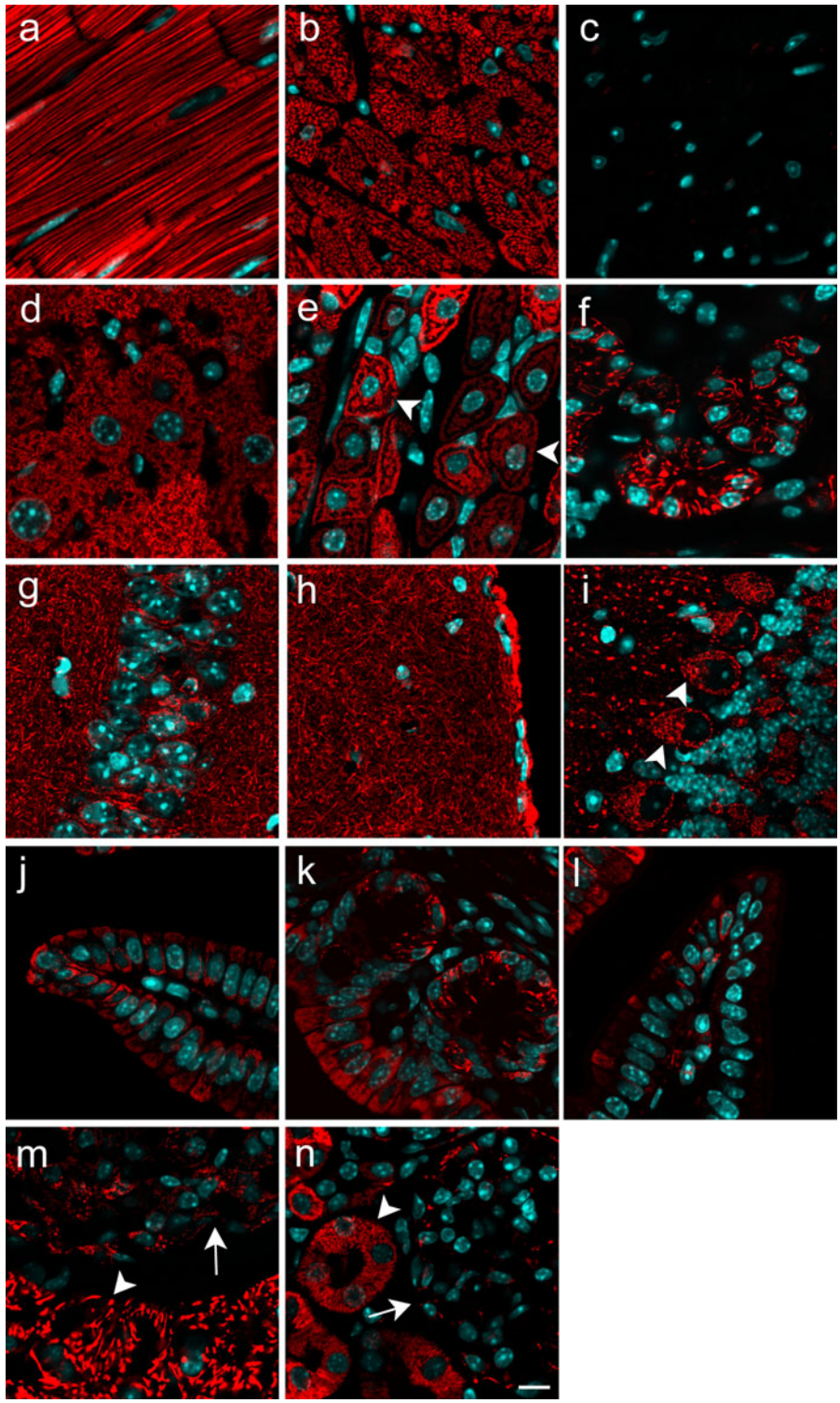
a
b
c
d
e
f
g
h
i
j
k
l
m
n

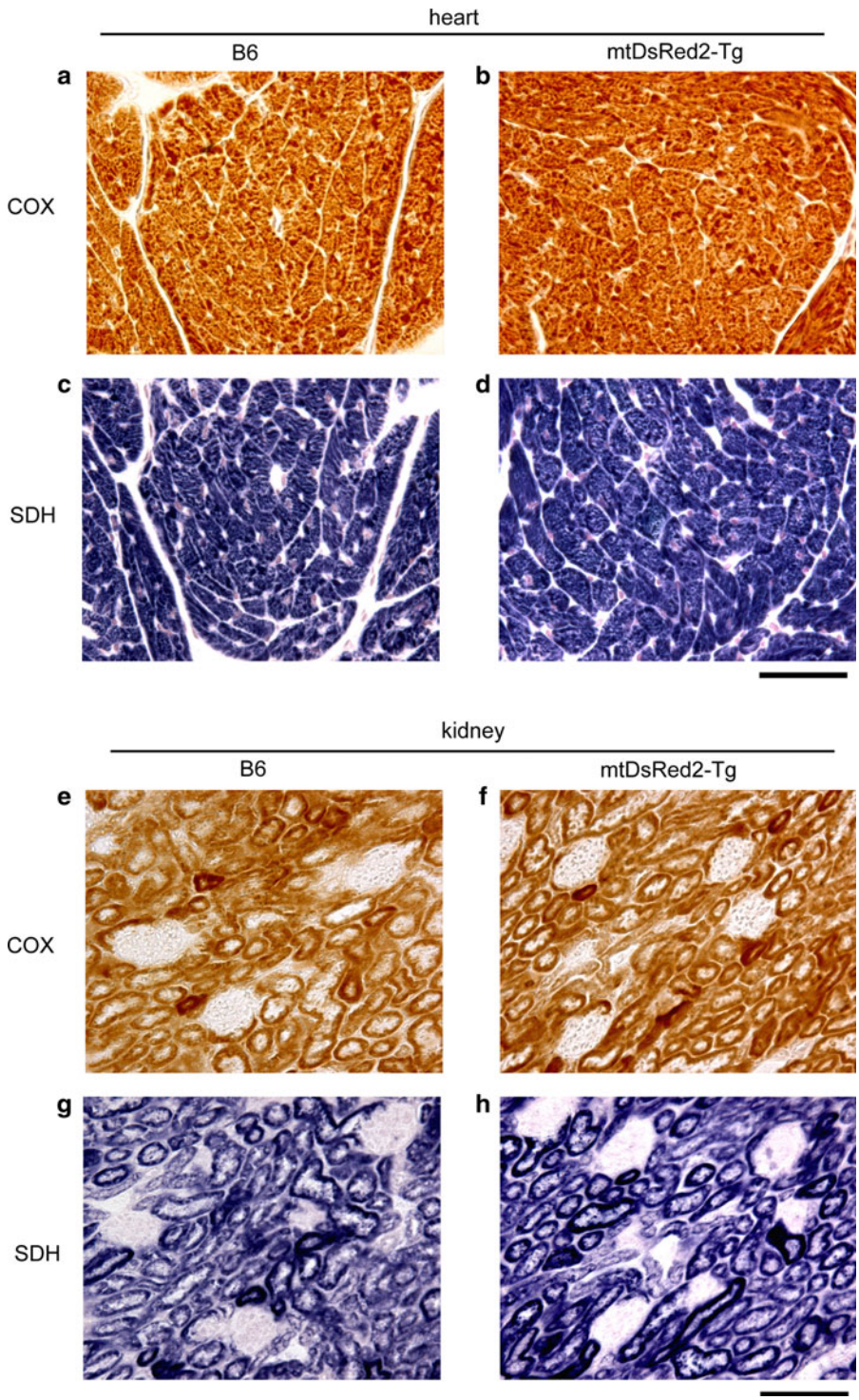

Fig. 3 Histochemical analyses of COX and SDH activities in an mtDsRed2-Tg mouse strain and a wild B6 mouse strain. COX-positive cells (*brown*) (**a**, **b**, **e**, **f**) and SDH-positive cells (*blue*) (**c**, **d**, **g**, **h**) were observed in the heart and kidney. *Scale bar* 50 μm (heart) and 100 μm (kidney)

conditions in mice (Chen et al. 2007). The mtDsRed2-Tg mouse strain could be useful in revealing a relationship between a defect in mitochondrial morphology and neurodegeneration, when used in combination with a mouse model for neurodegeneration. Mucosal epithelial cells of the ileum and colon

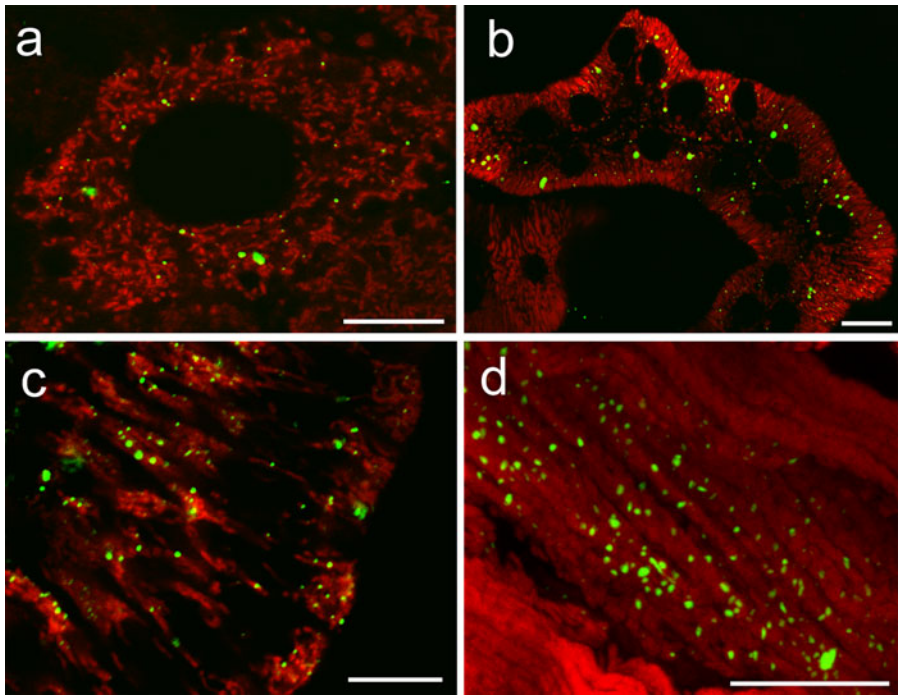

Fig. 4 DTg mice, generated by crossing mtDsRed2-Tg mice with *Tfam*/EGFP-Tg mice, allowing the simultaneous visualization of mitochondria (*red*) and mitochondrial nucleoids (*green*). Mitochondrial nucleoids were observed as punctate spots. **a** Liver cells. **b** Convoluted tubules in the kidney. **c** Mucosal epithelial cells of the ileum. **d** Longitudinal section of cardiac muscle fiber (3-dimensional image). *Scale bar* 10 μm

exhibited thread-shaped mitochondria (Fig. 2j, k). However, in intestinal villi of the ileum, the expression level of DsRed2 was not uniform (Fig. 2l). This differential expression level of DsRed2 was probably due to the different promoter activities in individual cells. In pancreatic acinar cells, mitochondria exhibited strong fluorescent intensity (Fig. 2m). In convoluted tubules of the kidney, a regular mitochondrial arrangement with high density was observed (Fig. 2n). These results were consistent with those of previous studies using mtGFP-Tg mice (Shitara et al. 2010). We found that the mtDsRed2-Tg mice outperforms mtGFP-Tg mice, as the frozen tissue sections from mtDsRed2-Tg mice provided better mitochondrial images than those provided by frozen tissue sections from mtGFP-Tg mice. The red fluorescent protein is excited and emits at longer wavelengths; therefore, autofluorescence can be reduced at these spectra (Miyawaki et al. 2003).

To assess the mitochondrial activity in the mtDsRed2-Tg mouse strain, histochemical analyses of COX and SDH activities were performed in the tissues (kidney and heart). When tissue sections from both the wild-type B6 and the mtDsRed2-Tg mouse strains were stained, no large differences in the activities of COX and SDH were observed between wild type and mtDsRed2-Tg (Fig. 3).

Then, the mtDsRed2-Tg mice were mated with *Tfam*/EGFP-Tg mice, which can be used to visualize mitochondrial nucleoids. Double-Tg mice (DTg mice), in which both transgenes are hemizygous, permit the simultaneous visualization of mitochondria and mitochondrial nucleoids. To detect these signals in various tissues, we prepared tissue sections and imaged mitochondria and mitochondrial nucleoids by confocal laser-scanning microscope, as described previously. As shown in Fig. 4, mitochondria and mitochondrial nucleoids were easily visualized in any tissue (liver, kidney, ileum, and heart tissues) in the DTg mice. Punctate green fluorescent signals were detected in the cells of tissues in a similar fashion as observed in cultured cells (Garrido et al. 2003). Some large mitochondrial nucleoids were observed in several tissues, which might have reflected the effect of *Tfam* over-expression as previously reported (Ylikallio et al. 2010). We also found that fluorescent

intensities of both DsRed2 and EGFP were not uniform in some cells and that in some regions, only one of the fluorescent proteins was detected. This might be because the two Tg promoters compete with each other for transcription factor(s).

EGFP has been widely used for examining the localization and dynamics of proteins, and the utilization of EGFP has revolutionized imaging technology in cell biology (Shaner et al. 2005; Tsien 1998). Recently, similar to *Tfam*/EGFP-Tg mice, several model mice in which proteins were visualized by EGFP were reported. For example, GFP-LC3 mouse strain expressing EGFP fused to LC3 was used to visualize autophagy (Mizushima et al. 2004), and GFP-actin mouse strain expressing GFP or EGFP fused to actin was generated to visualize microfilaments (Fischer et al. 2000; Gurniak and Witke 2007). By crossing the mtDsRed2-Tg mouse strain with these strains, mitochondria and these proteins can be morphologically analyzed.

We established the mtDsRed2-Tg mouse strain expressing mitochondrially tagged DsRed2 and characterized its expression pattern in living cells and tissues. Our results indicated that DsRed2 was expressed in mitochondria exclusively, and mitochondria were visualized in living, differentiated cells and tissues. Additionally, we obtained DTg mice by crossing mtDsRed2-Tg mice with *Tfam*/EGFP-Tg mice to simultaneously visualize mitochondria and mitochondrial nucleoids, and these signals were clearly observed in all examined tissues. Therefore, the mtDsRed2-Tg mice can be a valuable tool to examine interactions between mitochondria and EGFP-tagged proteins in living or fixed cells and tissues.

Acknowledgments We would like to thank Dr. J. Miyazaki for providing pCAGGS, Dr. L. Cao for valuable comments. This study was supported by Grants-in-Aid for Scientific Research (A) and (S) (to H. Yonekawa and J.-I. Hayashi), for Challenging Exploratory Research (to H. Yonekawa), and for Young Scientists (A) (to H. Shitara) from the Japan Society for the Promotion of Science and the Ministry of Education, Culture, Sports, Science, and Technology and by the Takeda Science Foundation research grant (to H. Yonekawa).

References

Alam TI, Kanki T, Muta T, Ukaji K, Abe Y, Nakayama H, Takio K, Hamasaki N, Kang D (2003) Human mitochondrial DNA is packaged with TFAM. Nucleic Acids Res 31(6):1640–1645

Chan DC (2006) Mitochondria: dynamic organelles in disease, aging, and development. Cell 125(7):1241–1252

Chen XJ, Butow RA (2005) The organization and inheritance of the mitochondrial genome. Nat Rev Genet 6(11): 815–825

Chen H, Chan DC (2006) Critical dependence of neurons on mitochondrial dynamics. Curr Opin Cell Biol 18(4): 453–459

Chen H, Detmer SA, Ewald AJ, Griffin EE, Fraser SE, Chan DC (2003) Mitofusins Mfn1 and Mfn2 coordinately regulate mitochondrial fusion and are essential for embryonic development. J Cell Biol 160(2):189–200

Chen H, McCaffery JM, Chan DC (2007) Mitochondrial fusion protects against neurodegeneration in the cerebellum. Cell 130(3):548–562

Fischer M, Kaech S, Wagner U, Brinkhaus H, Matus A (2000) Glutamate receptors regulate actin-based plasticity in dendritic spines. Nat Neurosci 3(9):887–894

Garrido N, Griparic L, Jokitalo E, Wartiovaara J, van der Bliek AM, Spelbrink JN (2003) Composition and dynamics of human mitochondrial nucleoids. Mol Biol Cell 14(4): 1583–1596

Griparic L, van der Wel NN, Orozco IJ, Peters PJ, van der Bliek AM (2004) Loss of the intermembrane space protein Mgm1/OPA1 induces swelling and localized constrictions along the lengths of mitochondria. J Biol Chem 279(18):18792–18798

Gurniak CB, Witke W (2007) HuGE, a novel GFP-actin-expressing mouse line for studying cytoskeletal dynamics. Eur J Cell Biol 86(1):3–12

Hasuwa H, Muro Y, Ikawa M, Kato N, Tsujimoto Y, Okabe M (2010) Transgenic mouse sperm that have green acrosome and red mitochondria allow visualization of sperm and their acrosome reaction in vivo. Exp Anim 59(1):105–107

Hermann GJ, Shaw JM (1998) Mitochondrial dynamics in yeast. Annu Rev Cell Dev Biol 14:265–303

Hirokawa N (1998) Kinesin and dynein superfamily proteins and the mechanism of organelle transport. Science 279(5350):519–526

Ishihara N, Nomura M, Jofuku A, Kato H, Suzuki SO, Masuda K, Otera H, Nakanishi Y, Nonaka I, Goto Y, Taguchi N, Morinaga H, Maeda M, Takayanagi R, Yokota S, Mihara K (2009) Mitochondrial fission factor Drp1 is essential for embryonic development and synapse formation in mice. Nat Cell Biol 11(8):958–966

Kroemer G, Reed JC (2000) Mitochondrial control of cell death. Nat Med 6(5):513–519

Larsson NG, Garman JD, Oldfors A, Barsh GS, Clayton DA (1996) A single mouse gene encodes the mitochondrial transcription factor A and a testis-specific nuclear HMG-box protein. Nat Genet 13(3):296–302

Matsuda N, Sato S, Shiba K, Okatsu K, Saisho K, Gautier CA, Sou YS, Saiki S, Kawajiri S, Sato F, Kimura M, Komatsu M, Hattori N, Tanaka K (2010) PINK1 stabilized by mitochondrial depolarization recruits Parkin to damaged mitochondria and activates latent Parkin for mitophagy. J Cell Biol 189(2):211–221

Misgeld T, Kerschensteiner M, Bareyre FM, Burgess RW, Lichtman JW (2007) Imaging axonal transport of mitochondria in vivo. Nat Methods 4(7):559–561

Miyawaki A, Sawano A, Kogure T (2003) Lighting up cells: labelling proteins with fluorophores. Nat Cell Biol (Suppl) 5:S1–S7

Mizushima N, Yamamoto A, Matsui M, Yoshimori T, Ohsumi Y (2004) In vivo analysis of autophagy in response to nutrient starvation using transgenic mice expressing a fluorescent autophagosome marker. Mol Biol Cell 15(3): 1101–1111

Nishiyama S, Shitara H, Nakada K, Ono T, Sato A, Suzuki H, Ogawa T, Masaki H, Hayashi JI, Yonekawa H (2010) Over-expression of Tfam improves the mitochondrial disease phenotypes in a mouse model system. Biochem Biophys Res Commun 401(1):26–31

Niwa H, Yamamura K, Miyazaki J (1991) Efficient selection for high-expression transfectants with a novel eukaryotic vector. Gene 108(2):193–199

Ono T, Isobe K, Nakada K, Hayashi JI (2001) Human cells are protected from mitochondrial dysfunction by complementation of DNA products in fused mitochondria. Nat Genet 28(3):272–275

Rizzuto R, Brini M, Pizzo P, Murgia M, Pozzan T (1995) Chimeric green fluorescent protein as a tool for visualizing subcellular organelles in living cells. Curr Biol 5(6):635–642

Rizzuto R, Bernardi P, Pozzan T (2000) Mitochondria as all-round players of the calcium game. J Physiol 529(Pt 1): 37–47

Sachs G, Chang HH, Rabon E, Schackman R, Lewin M, Saccomani G (1976) A nonelectrogenic H+ pump in plasma membranes of hog stomach. J Biol Chem 251(23): 7690–7698

Seligman AM, Karnovsky MJ, Wasserkrug HL, Hanker JS (1968) Nondroplet ultrastructural demonstration of cytochrome oxidase activity with a polymerizing osmiophilic reagent, diaminobenzidine (DAB). J Cell Biol 38(1):1–14

Shaner NC, Steinbach PA, Tsien RY (2005) A guide to choosing fluorescent proteins. Nat Methods 2(12):905–909

Shitara H, Kaneda H, Sato A, Iwasaki K, Hayashi JI, Taya C, Yonekawa H (2001) Non-invasive visualization of sperm mitochondria behavior in transgenic mice with introduced green fluorescent protein (GFP). FEBS Lett 500(1–2): 7–11

Shitara H, Shimanuki M, Hayashi JI, Yonekawa H (2010) Global imaging of mitochondrial morphology in tissues using transgenic mice expressing mitochondrially targeted enhanced green fluorescent protein. Exp Anim 59(1): 99–103

Tsien RY (1998) The green fluorescent protein. Annu Rev Biochem 67:509–544

Yaffe MP (1999) Dynamic mitochondria. Nat Cell Biol 1(6):E149–E150

Ylikallio E, Tyynismaa H, Tsutsui H, Ide T, Suomalainen A (2010) High mitochondrial DNA copy number has detrimental effects in mice. Hum Mol Genet 19(13):2695–2705